IJCA

Indonesian Journal of Chemical Analysis

Homepage: https://journal.uii.ac.id/IJCA

Photocatalytic Activity of ZnO Nanoparticles Synthesized Using *Persea* sp. Leaf Extract Toward Methylene Blue Dye Degradation

Ryanna Nathania Simbolon, Demi Dama Yanti*, I Putu Mahendra, Aditya Ayuwulanda, Rahmat Kurniawan, Cindy Moyna Clara L. A., Gabriell Vannes Sabat Tuta

Chemistry Study Program, Deparment of Science, Institut Teknologi Sumatera, Indonesia
*Corresponding author: demi.damayanti@ki.itera.ac.id
DOI: 10.20885/ijca.vol8.iss2.art4

GRAPHICAL ABSTRACT

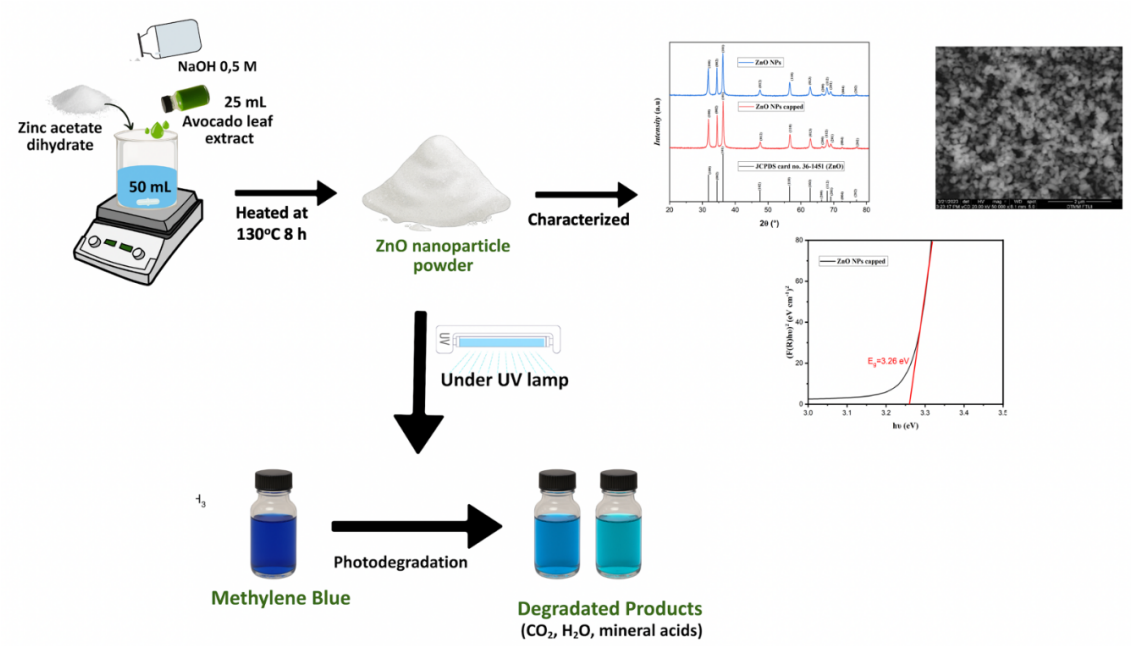

ARTICLE INFO

Received : 15 July 2025
Revised : 21 August 2025
Published : 29 September 2025
Keywords : Methylene blue, ZnO NPs, Green synthesis, *Persea* sp. leaf extract, Photocatalytic degradation

ABSTRACT

Methylene blue dye is widely used in various industries, but improper disposal can severely harm aquatic ecosystems. Zinc oxide (ZnO), a well-known semiconductor, is frequently employed to degrade dye pollutants in aqueous media. This study synthesized ZnO nanoparticles via a precipitation method incorporating a green synthesis approach, utilizing Persea sp (*Persea* sp.) leaf extract as an eco-friendly alternative to synthetic chemical reagents. Persea sp leaves contain diverse secondary metabolites, including saponins, alkaloids, tannins, flavonoids, and phenolics, which act as capping agents during water-based synthesis. Characterization was conducted using X-ray diffraction (XRD), UV–visible diffuse reflectance spectroscopy (UV-DRS), and scanning electron microscopy (SEM). The photocatalytic activity of the ZnO nanoparticles toward methylene blue degradation was evaluated under UV irradiation at time intervals

of 10, 20, 30, 40, 50, and 60 minutes. UV-DRS results indicated a maximum absorption wavelength of 364 nm with a band gap energy of 3.26 eV. XRD analysis confirmed a hexagonal wurtzite structure (JCPDS no. 36-1451) with an average crystallite size of 21.24 nm. SEM imaging revealed a nanospherical morphology with an average particle size of 79.28 nm. The synthesized ZnO nanoparticles achieved 61.77% degradation efficiency for 5 ppm methylene blue. These findings demonstrate that green-synthesized ZnO nanoparticles from *Persea* sp. leaf have promising potential as sustainable photocatalysts for dye removal, contributing to the development of environmentally friendly wastewater treatment technologies.

1. INTRODUCTION

Methylene blue (MB), with the molecular formula $C_{16}H_{18}N_3ClS$, is a basic aromatic heterocyclic dye that has a wavelength range of 550 nm - 663 nm [1, 2]. MB is commonly used in industry to dye silk, wool, cotton, and paper. This dye generates by-products in liquid waste, which must be appropriately treated before being discharged into the environment. Improperly managed, MB-containing wastewater may cause skin irritation, organ damage, toxicity to aquatic organisms, and potentially carcinogenic effects [3, 4]. Alternative solutions have been proposed to overcome these issues, including using metal oxide nanoparticles as photocatalysts to degrade dye pollutants.

In recent years, researchers have grown interested in nanoparticles due to their unique physicochemical properties. Nanoparticles are solid colloidal particles with diameters ranging from 10 to 100 nm, and may contain various chemical compounds [5]. Numerous metal oxide nanoparticles are being investigated, including CaO [6], MgO [7], TiO_2 [8], Fe_3O_4 [9], and ZnO [10]. Among these, ZnO nanoparticles are particularly popular due to their advantages, such as cost-effectiveness, easy availability, and non-toxic properties [11, 12]. ZnO nanoparticles are semiconductor n-type materials with a band gap of about 3.26 eV at room temperature [13]. ZnO nanoparticles have diverse applications in everyday life, including gas sensors, antibacterial agents, antidiabetic treatments, antioxidants, biosensors, optical and electrical devices, solar cells, and photocatalysts [14, 15]. In previous research, the application of ZnO nanoparticles has been extensively evaluated as photocatalysts for the degradation of dyes such as rhodamine B, congo red, and naphthol blue black [13, 16, 17].

ZnO nanoparticles can be synthesized via several methods, including ultrasound, precipitation, sol-gel, solvothermal, hydrothermal, and more. Recently, there has been growing interest in developing environmentally friendly or green synthesis approaches. Substituting some synthetic chemicals with natural materials is one step in implementing green synthesis principles [18, 19]. Previous studies have reported the successful synthesis of ZnO nanoparticles using plant extracts rich in secondary metabolites, such as polyphenols, polysaccharides, terpenoids, flavonoids, and alkaloids, which act as effective reducing and capping agents. For example, Yanti et al. synthesized zinc oxide nanoparticles using *Crescentia cujete* L. leaf extract, while Gao et al. employed *Limonium pruinosum* L. Chaz. extract. Both studies yielded nanoparticles with unique properties [10, 20].

Persea sp is one of the agricultural commodities cultivated in Lampung Province. Previous studies have reported that Persea sp leaf extract contains various bioactive compounds, including saponins, alkaloids, tannins, and flavonoids [21], which may serve as capping agents during nanoparticle synthesis. Saridewi et al. prepared ZnO nanoparticles using Persea sp seed extract for antibacterial activity tests [22]. Vinay et al. synthesized silver nanoparticles using Persea sp leaf extract to evaluate their antibacterial effects [23]. However, to our knowledge, no studies have investigated the use of Persea sp leaf extract as a capping agent for the synthesis of ZnO nanoparticles; previous work has focused only on Persea sp seeds, while the leaves have been applied exclusively to silver nanoparticle synthesis.

Based on these considerations, the present study focuses on the green synthesis of ZnO nanoparticles using Persea sp leaf extract as the capping agent. The aim of this research is to determine whether ZnO nanoparticles can be formed using Persea sp leaf extract and to evaluate their

photocatalytic activity in the degradation of methylene blue, a common organic dye used in the textile industry. Precipitation was selected as the synthesis method, and the resulting nanoparticles were characterized using XRD, SEM, and UV–DRS. Preliminary experiments were conducted to establish whether the synthesized ZnO nanoparticles could be applied as photocatalysts for the degradation of methylene blue by analyzing the effect of contact time (10, 20, 30, 40, 50, and 60 min). Figure 1 illustrates of the overall research framework.

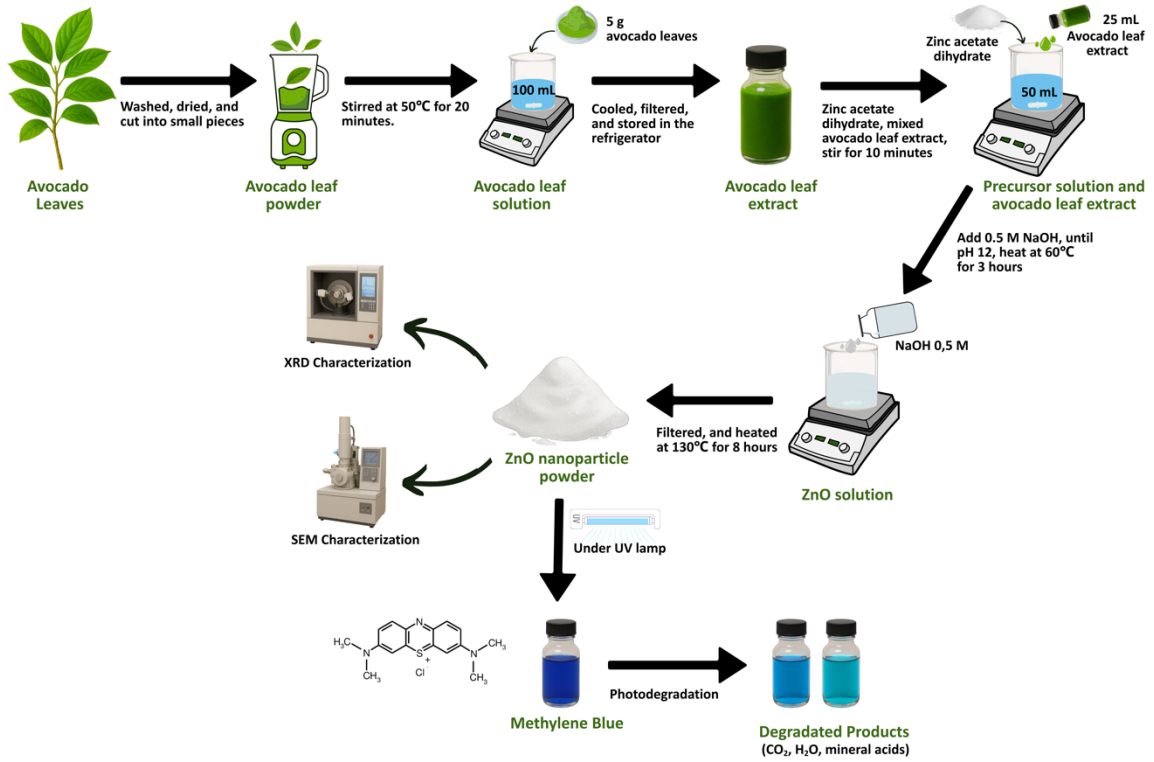

Figure 1. Schematic representation of the entire study.

2. EXPERIMENTAL METHODS

2.1. Materials

Persea sp leaves were collected from Griya Sukarame Housing, Lampung, Indonesia. The leaves were transported to the laboratory immediately for synthesis. Zinc acetate dihydrate ($Zn(CH_3CO_2)_2.2H_2O$) and methylene blue were purchased from Merck, and all are of research grade. Distilled water was used as a solvent during the biosynthesis process. All the chemicals were used without any further purification.

2.2. Instrumentation

The powder of ZnO nanoparticles was characterized to determine the properties of the synthesized ZnO nanoparticles. The characterization techniques performed include XRD, SEM, and Uv-Vis DRS. The formation of ZnO nanoparticles was confirmed by X-Ray Diffraction (XRD-Malvern Panalytical) with Cu Kα as radiation source, operated within a radiation angle of 20 to 80°. The surface morphology and size of ZnO nanoparticles were observed using a Scanning Electron Microscope (SEM-INSPECT F50) with magnifications of 25000, 50000, 100000, and 200000. The band gap between the valence band and the conduction band was determined by UV-DRS (Agilent Technologies). All the characterization was carried out at the Metallurgical and Materials Laboratory, University of Indonesia.

2.3. Procedure

Extraction of Persea sp

The green and fresh *Persea sp* leaf extract was rinsed with running and distilled water to remove foreign particles. The leaf was then dried at room temperature to remove the washing water.

The clean and dry *Persea sp* leaves were then cut into pieces and chopped into fine particles. 5 g of *Persea sp* leaf were heated in 100 mL of distilled water at 50 °C for 20 minutes. The extract was then filtered using filter paper and stored in a cool, dry place for further use.

Qualitative phytochemical screening of Persea sp leaf extract

In this study, a simple phytochemical screening was conducted to identify the secondary metabolite compounds present in the crude extract of a *Persea sp* leaf. The tests carried out in this research are flavonoid, phenolic, tannin, and saponin tests. The method of phytochemical test was adopted from previous research [10].

Flavonoid test

Two methods were used in this flavonoid test. The first method followed the Wilstater technique, where approximately 5 mL of crude *Persea sp* leaf extract was placed in a 10 mL vial, adding 5 drops of concentrated HCl solution and a strip of Mg. A color change to orange-pink indicates a positive result for flavonoids. The second method involved adding 10% NaOH to 5 mL of the crude *Persea sp* leaf extract. A color change to reddish-brown indicates a positive result for flavonoids.

Phenolic test

About 5 mL of crude *Persea sp* leaf extract was mixed with a few drops of 1% $FeCl_3$ solution. A color change to blackish-blue confirms the presence of phenols.

Tannin test

5 mL of crude *Persea sp* leaf extract was combined with a few drops of 1% $FeCl_3$ solution and then heated to a boil on a hotplate. A color change to blackish-blue was taken as a positive test for tannins.

Saponin test

Approximately 5 mL of crude *Persea sp* leaf extract was placed in a 10 mL vial and shaken until abundant foam formed. Afterward, HCl was added, and the mixture was left to stand for 15 minutes. The Persea sp leaf extract tests positive for saponins if the foam remains stable.

Synthesis ZnO nanoparticles

ZnO nanoparticles were synthesised via precipitation, following a previously reported procedure with slight modifications [10]. In a typical synthesis, 50 mL of a 0.2 M Zn^{2+} precursor solution was transferred into a beaker, and 25 mL of *Persea* sp. leaf extract was added. The mixture was stirred at room temperature for 10 minutes. Subsequently, 0.5 M NaOH was added dropwise until the pH reached 9. The resulting suspension was continuously stirred at 60 °C for 3 hours. The precipitate formed at the bottom of the beaker was separated using Whatman No.42 filter paper. The obtained white solid was washed with distilled water and ethanol, and then dried at 130 °C for 8 hours. XRD, SEM, and UV–Vis DRS characterized the resulting pale greenish powder.

Photocatalytic evaluation of ZnO nanoparticles towards methylene blue dye

The photocatalytic activity of the synthesised ZnO nanoparticles was evaluated based on the procedure reported by Vihayakumar et al., with slight modifications [24]. In a typical experiment, 50 mg of the ZnO nanoparticles were dispersed in 20 mL of a 5 ppm methylene blue solution. The suspension was kept in the dark for 60 minutes to establish adsorption–desorption equilibrium. Afterward, a 5 mL aliquot was withdrawn, transferred into a centrifuge tube, and centrifuged at 6000 rpm for 10 minutes. The remaining suspension was then exposed to a UV lamp for various irradiation times (10, 20, 30, 40, 50, and 60 minutes). After each irradiation period, aliquots were collected and centrifuged under the same conditions as the non-irradiated sample. The supernatants were subsequently analysed using a UV–Vis spectrophotometer within the wavelength range of 200–700 nm.

3. RESULTS AND DISCUSSIONS

3.2. Qualitative Phytochemical Screening of *Persea sp* Leaf and Synthesis ZnO Nanoparticles

The green leaves of *Persea sp* were extracted using water at low temperature. The low

temperature was chosen to prevent the breakdown of the secondary metabolites contained in the leaf. Qualitative phytochemical screening confirmed the presence of secondary metabolites, which can be a capping agent in synthesizing ZnO nanoparticles.

TABLE I. Secondary metabolites contains in the leaf of *Persea sp.*

Secondary metabolites	Test reagent	Positive Result	Result
Saponins	Distilled water	Stable foam after 10 minutes	-
Tannins	$FeCl_3$	Greenish – black solution	+
Flavonoids	NaOH	Yellowish – brown solution	+
	HCl + Mg	Pink solution	+
Phenolics	$FeCl_3$	Blackish – blue solution	+

Table 1 summarises the phytochemical screening results of *Persea* sp. leaf extract. The water extract of *Persea* sp. leaf has a pale yellow color. The extract tested negative for saponins, as indicated by the absence of stable foam when the extract was shaken. The color change of the extract when combined with 1% $FeCl_3$ suggested the presence of tannins as secondary metabolites. Furthermore, the extract contained flavonoids, as confirmed by tests using two different reagents; both tests showed positive results. The extract also contained phenolics, as evidenced by the color change from pale yellow to bluish-black. According to the qualitative phytochemical screening, the extract was positive for flavonoids, phenolics, and tannins, as shown in Figure 2.

Figure 2. Phytochemical screening of *Persea sp* leaf extract.

FTIR analysis has been carried out based on previous studies on *Persea* sp. leaf aqueous extract. The FTIR results confirmed the presence of several functional groups in the extract, namely –OH, $–NH_2$, –C=O, –C–O, –C–H, and $–CH_2$ [25]. These findings further support the presence of secondary metabolites identified through the phytochemical screening carried out in the present study. One of the key functional groups present in flavonoids is the hydroxyl (–OH) group. The hydroxyl (–OH) groups from the secondary metabolites in the leaf extract interact electrostatically with the Zn^{2+} precursor. These hydrophilic –OH groups surround the Zn^{2+} ions, thus controlling particle growth and preventing agglomeration [26]. The formation of ZnO proceeds according to reactions (1) and (2), while the role of organic compounds in the secondary metabolites is illustrated in Fig. 3. Based on Fig. 3, the secondary metabolites contained in *Persea* sp. leaf extract act as bioreductors and also protect the ZnO particles from contacting each other. This condition leads to a good particle size distribution and maintains the particle size within the nanoscale range. ZnO nanoparticles synthesized without a capping agent do not receive protection between individual particles, resulting in less controlled particle growth and consequently larger particle sizes than nanoparticles synthesized in the presence of a capping agent [27].

$$Zn(CH_3COO)_2(aq) + 2NaOH(aq) \rightarrow Zn(OH)_2(s) + 2CH_3COONa(aq) + 2H_2O(l) \quad (1)$$

$$Zn(OH)_2(s) \rightarrow ZnO(s) + H_2O(g) \quad (2)$$

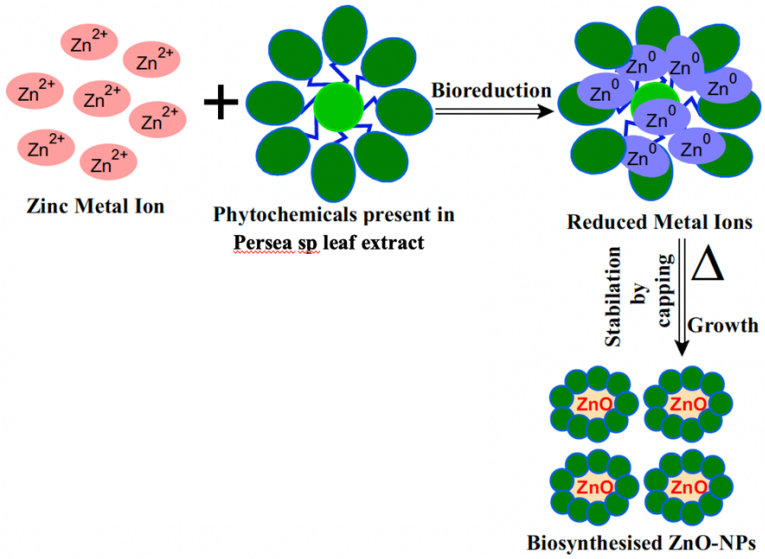

Figure 3. Schematic role of *Persea* sp. secondary metabolites as capping agents [27].

3.3. Characterization of ZnO Nanoparticles

3.3.1. XRD Analysis

The X-ray diffraction (XRD) patterns of ZnO nanoparticles, both with and without a capping agent, exhibited diffraction peaks at 2θ values of 31.83°, 34.47°, 36.33°, 47.61°, 56.68°, 62.91°, 66.47°, 68.01°, 69.15°, and 89.63°. These peaks correspond to the Miller indices (100), (002), (101), (012), (110), (013), (200), (112), (201), and (203), respectively, as referenced in the Joint Committee on Powder Diffraction Standards (JCPDS) database No. 36-1451. The data revealed a sharp and intense diffraction peak within the 2θ range of 30° – 40°, indicating a well-defined crystalline structure [28].

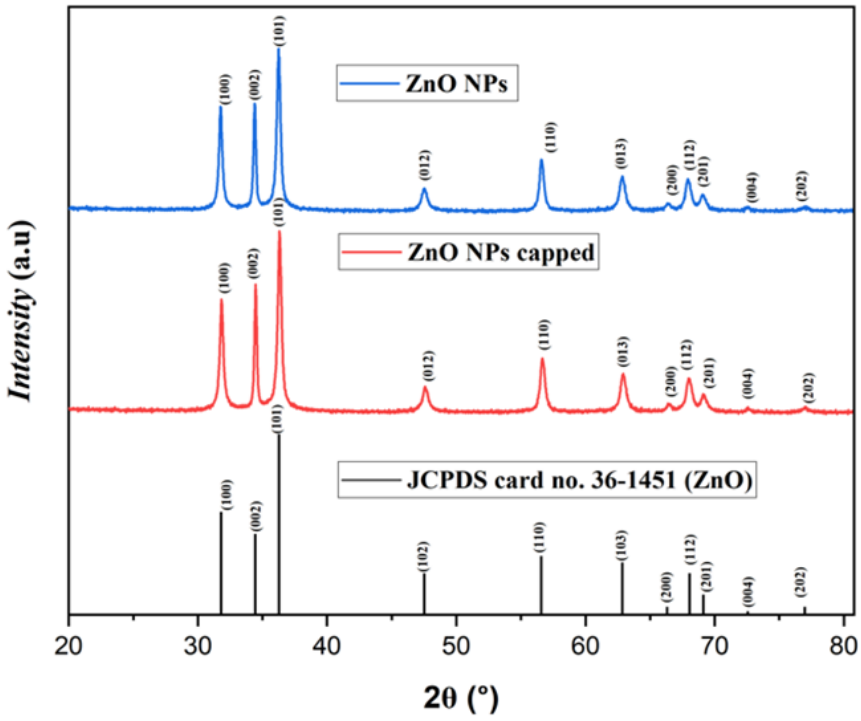

Figure 4. XRD patterns of the capped and non-capped ZnO nanoparticles.

The XRD pattern of the synthesised ZnO nanoparticles confirms a wurtzite crystal structure with a hexagonal phase. As depicted in Fig. 4, the XRD diffractogram exhibits the absence of impurity peaks, indicating the high purity of the ZnO sample. According to the XRD results, the ZnO

nanoparticles are predicted to crystallise perfectly. There are no different peaks between ZnO synthesised using a capping agent and without a capping agent; both diffractograms show peaks at the same 2θ values. The average crystallite size of the ZnO nanoparticles synthesised using a capping agent is calculated using Debye–Scherrer's equation [29] and found to be 21.24 nm. ZnO nanoparticles synthesised without a capping agent have an average crystallite size of about 22.41 nm. The difference in the size of the ZnO nanoparticles is attributed to the stabilisation effect provided by the capping agent added during the synthesis process. The crystallite size of ZnO nanoparticles synthesised with *Persea* sp. leaf extract as a capping agent is smaller than that of nanoparticles synthesised without a capping agent. This result suggests an interaction between Zn^{2+} precursors and *Persea* sp. leaf extract.

3.3.2. SEM Analysis

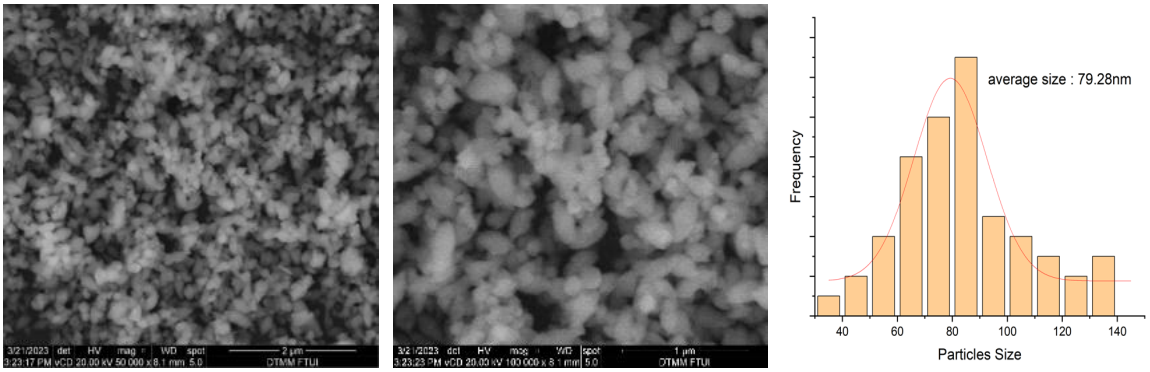

(a) **(b)** **(c)**

Figure 5. SEM image of the synthesized ZnO nanoparticles at magnification of 50.000 (a), 100.000 (b), and Average size of the synthesized ZnO nanoparticles.

Scanning electron microscopy (SEM) is used to analyse the surface morphology, shape, and size of the synthesised ZnO nanoparticles. Figure 5(a) and (b) depict the SEM image of ZnO, showing a predominantly spherical morphology with slight agglomeration. The observed slight agglomeration may result from strong interparticle forces due to the high surface energy of ZnO in the nanoscale. The slight agglomeration may also be caused by the presence of residual extract during the synthesis process [26]. Additionally, the surface texture of the nanoparticles appears relatively smooth, suggesting a uniform synthesis process.

Figure 5(c) presents the size distribution of the ZnO nanoparticles. The x-axis represents the particle size distribution, while the y-axis shows the number of particles with a specific size. Based on this diagram, it can be observed that the ZnO nanoparticles exhibit a predominant size range between 80 and 90 nm. The particles are uniformly distributed, with an average size of approximately 79.28 nm, as depicted in Figure 5(c). According to the general definition, the synthesised ZnO particles are considered nanoparticles, since their average size is less than 100 nm.

3.4. UV-DRS Analysis

UV–Vis DRS is performed to identify the band gap energy of the synthesised ZnO nanoparticles [30]. The band gap energy is important because it determines the ability of ZnO to excite electrons from the valence band to the conduction band. This electron excitation leads to the formation of holes within the ZnO nanoparticles. The maximum absorbance wavelength is measured within the range of 200–800 nm. Based on the literature, ZnO nanoparticles exhibit absorbance at 350–380 nm [31]. Figure 6(a) depicts the absorbance wavelength of the ZnO nanoparticles, which is detected at 364 nm. This result is consistent with previous research, which reports the absorbance wavelength of ZnO nanoparticles at approximately 352 nm [32]. The UV–Vis DRS characterisation provides spectral data in the form of wavelength (λ), absorbance (A), and reflectance (R). The band gap energy is calculated using the Tauc plot method in conjunction with the Kubelka–Munk equation [33].

$$F(R) = \frac{K}{S} = \frac{(1-R)^2}{2R} \quad (1)$$

$$Eg = hv = \frac{hc}{\lambda} \quad (2)$$

Where R is reflectance ratio; K is molar absorption coefficient; S is scattering factor; Eg is gap energy; h is planck constant; and λ is wavelength. The Tauc Plot method is based on the assumption that the molar absorption coefficient (α) can be expressed using the following equation:

$$(\alpha.hv)^2 = B(hv - Eg) \quad (3)$$

F(R) was assumed to be equivalent with α, and the equation can be expressed as follows:

$$(F(R).hv)^2 = B(hv - Eg) \quad (4)$$

Where B is a constant linked to the material, and hv represents the photon energy. Figure 6(b) shows the Tauc plot of the ZnO nanoparticles, with the absorbance taken along the vertical axis and the energy taken on the horizontal axis. The optical band gap for the absorption peak is obtained by extending the linear portion of the $(\alpha hv)^2$–hv curve to zero. According to the plot, the band gap energy of the ZnO nanoparticles is about 3.26 eV. The band gap of the synthesised ZnO nanoparticles is aligned with an earlier report indicating that ZnO possesses a band gap of around 3.11–3.33 eV [30].

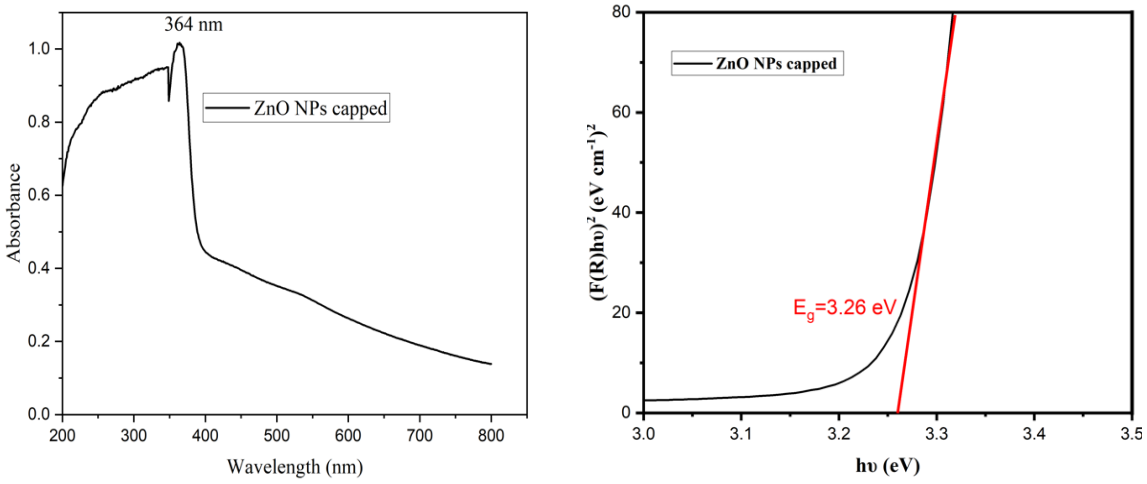

Figure 6. UV-DRS spectrum of the synthesized ZnO nanoparticles (a) and Tauc plot of the synthesized ZnO nanoparticles (b).

Photocatalityc Activity of ZnO Nanoparticles

The photocatalytic activity of synthesized ZnO nanoparticles was carried out using spectrophotometer Uv-Vis. The degradation percentage of methylene blue was measured using the equation:

$$\text{Degradation (\%)} = \frac{Co - C}{Co} \times 100\% \quad (5)$$

Where C_0 represents the initial concentration and C represents the remaining concentration of methylene blue. In this study, the maximum contact time is 60 minutes, and samples were taken every 10 minutes. Figure 7 depicts the degradation percentage of ZnO nanoparticles as a function of contact time. As the irradiation time increased to 60 minutes, the degradation percentage reached 61,77%, indicating a decrease in the concentration of methylene blue.

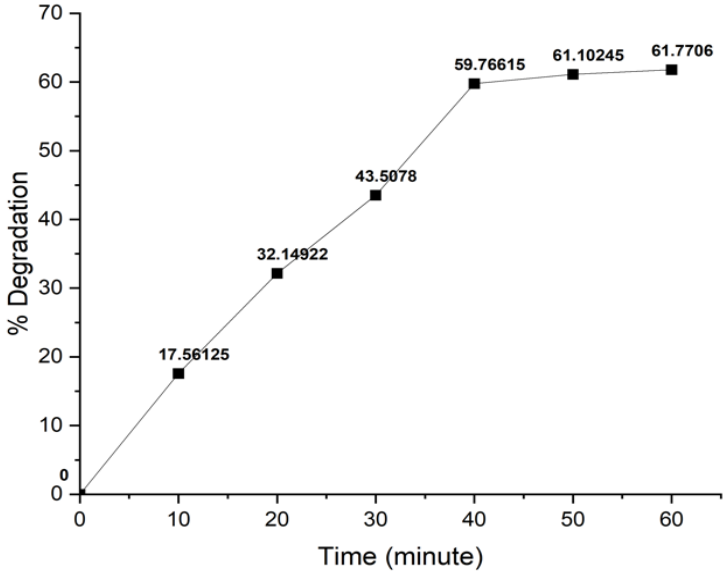

Figure 7. Photodegradation studies of the synthesized ZnO nanoparticles towards methylene blue.

The mechanism of ZnO nanoparticles as photocatalysts is illustrated in reactions (1) to (5) [34] and also schematic in Figure 8 [27]. When ZnO is exposed to UV light, the incident energy excites the electrons from the valence band to the conduction band. This excitation process generates electron–hole pairs, where the electrons (e^-) are transferred to the conduction band and leave behind holes (h^+) in the valence band. Subsequently, the photogenerated electrons react with dissolved oxygen at the ZnO surface to form superoxide radicals ($\bullet O_2^-$), while the holes react with adsorbed water molecules or hydroxide ions to produce highly oxidative hydroxyl radicals (•OH). These reactive oxygen species (ROS) initiate a series of oxidation reactions that degrade methylene blue molecules into smaller and less harmful products, such as CO_2 and H_2O. Therefore, the photocatalytic activity observed in this study is directly related to the generation of ROS during the ZnO excitation process [34].

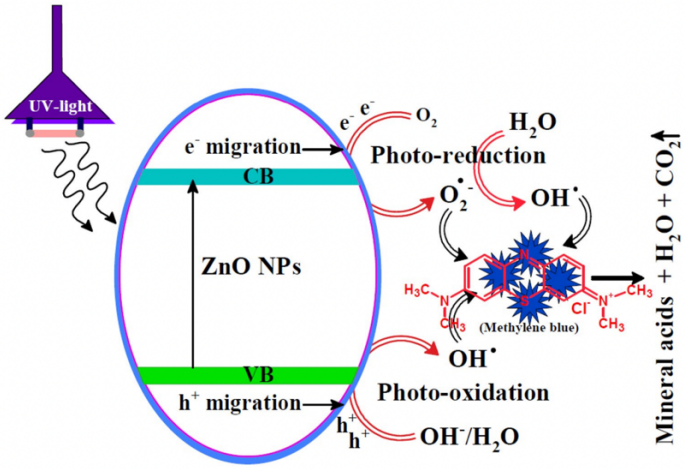

Figure 8. Schematic diagram of photocatalytic process of ZnO nanoparticles towards methylene blue degradation [27].

$$ZnO + h\nu \rightarrow ZnO\ (e^- + h^+) \quad (1)$$

$$h^+ + H_2O \rightarrow h^+ + OH\bullet \quad (2)$$

$$h^+ + OH^- \rightarrow \bullet OH \quad (3)$$

$$e^- + O_2 \rightarrow \bullet O_2^- \quad (4)$$

$$16\bullet OH + 31\bullet O_2^- + C_{16}H_{18}N_3ClS \rightarrow 16CO_2 + SO_4^{2-} + 3NO_3^- + Cl^- + H_2O \quad (5)$$

The degradation performance in this study was related to the previous reports in Table 2. Several factors influence the photocatalytic performance of nanoparticle ZnO, including dosage of material, pH of the solution, irradiation time, and concentration of dyes [35]. These parameters play a significant role in determining photocatalytic degradation efficiency, particularly in applications involving methylene blue. According to these results, the synthesized ZnO using *Persea sp* leaf extract demonstrates potential as a photocatalyst for methylene blue degradation.

TABLE II. Photocatalytic performance of ZnO nanoparticles against methylene blue.

No	Dosage (mg)	MB conc. (ppm)	Time (min)	Deg. (%)	Ref.
1	50	5	32	55.69	[35]
2	-	0.3	540	64	[36]
3	50	10	50	36.7	[10]
4	200	100	60	22.8	[37]
5	50	5	60	61	This research

In this study, the effect of irradiation time was investigated to explore the influence of irradiation time on the photocatalytic activity of ZnO nanoparticles. According to this study, a longer irradiation time allows continuous interaction between UV light and ZnO, resulting in increased reactive oxygen species (ROS) formation—the interaction between reactive oxygen species and methylene blue leads to a greater dye degradation.

4. CONCLUSIONS

The Persea sp. leaf extract successfully acted as a green capping agent in synthesizing ZnO nanoparticles. The synthesized nanoparticles were confirmed to possess a hexagonal wurtzite crystal structure with an average crystallite size of 21.24 nm, as determined by the Debye–Scherrer equation. SEM analysis revealed that the particles had an average size of 79.28 nm with a spherical morphology. The optical band gap of the synthesized ZnO nanoparticles was measured using UV-Vis DRS and found to be 3.26 eV. Furthermore, the ZnO nanoparticles demonstrated photocatalytic activity by degrading 5 ppm of methylene blue with an efficiency of 61.77%. Based on all characterization results and preliminary tests as a photocatalyst for the degradation of methylene blue dye using ZnO nanoparticles, this material is suitable for being considered as a candidate photocatalyst for methylene blue dye.

References

[1] B. Charmas, M. Zięzio, and K. Jedynak, "Assessment of the Porous Structure and Surface Chemistry of Activated Biocarbons Used for Methylene Blue Adsorption," *Molecules*, vol. 28, no. 13, p. 4922, Jun. 2023, doi: 10.3390/molecules28134922.

[2] J. Jiang *et al.*, "Rapid photodegradation of methylene blue by laser-induced plasma," *RSC Adv.*, vol. 12, no. 33, pp. 21056–21065, 2022, doi: 10.1039/d2ra03633a.

[3] I. Khan *et al.*, "Review on Methylene Blue: Its Properties, Uses, Toxicity and Photodegradation," *Water*, vol. 14, no. 2, p. 242, Jan. 2022, doi: 10.3390/w14020242.

[4] P. O. Oladoye, T. O. Ajiboye, E. O. Omotola, and O. J. Oyewola, "Methylene blue dye: Toxicity and potential elimination technology from wastewater," *Results Eng.*, vol. 16, p. 100678, Dec. 2022, doi: 10.1016/j.rineng.2022.100678.

[5] A. Dubey and R. Gupta, "Nanoparticles: An Overview," vol. 10, no. 1, 2021.

[6] M. Ikram *et al.*, "Enhanced Photocatalytic Degradation with Sustainable CaO Nanorods Doped with Ce and Cellulose Nanocrystals: In Silico Molecular Docking Studies," *ACS Omega*, vol. 7, no. 31, pp. 27503–27515, Aug. 2022, doi: 10.1021/acsomega.2c02732.

[7] M.-A. Gatou *et al.*, "Optimization of ZnO Nanoparticles' Synthesis via Precipitation Method Applying Taguchi Robust Design," *Catalysts*, vol. 13, no. 10, p. 1367, Oct. 2023, doi: 10.3390/catal13101367.

[8] M.-A. Gatou, A. Syrrakou, N. Lagopati, and E. A. Pavlatou, "Photocatalytic TiO2-Based Nanostructures as a Promising Material for Diverse Environmental Applications: A Review," *Reactions*, vol. 5, no. 1, pp. 135–194, Feb. 2024, doi: 10.3390/reactions5010007.

[9] R. D. Ningtyas, D. D. Yanti, A. K. Amin, and A. Aji, "Fabrication of a Fe3O4/CS/AgNPs Composite from Indigenous Iron Sand for Enhanced Methylene Blue Adsorption," *J. Clust. Sci.*, vol. 35, no. 5, pp. 1463–1480, Jun. 2024, doi: 10.1007/s10876-024-02594-0.

[10] D. D. Yanti, S. Aprilia, B. Ariwahjoedi, M. A. Serunting, and H. P. C. A. Cane, "Biosynthesis of ZnO Nanoparticles Mediated by Crescentia cujete L Leaves Extract and The Photocatalytic Activities Towards Methylene Blue," *J. Kim. Sains Dan Apl.*, vol. 26, no. 12, pp. 457–465, Jan. 2024, doi: 10.14710/jksa.26.12.457-465.

[11] A. Baig, M. Siddique, and S. Panchal, "A Review of Visible-Light-Active Zinc Oxide Photocatalysts for Environmental Application," *Catalysts*, vol. 15, no. 2, p. 100, Jan. 2025, doi: 10.3390/catal15020100.

[12] S. A. Mousa, D. A. Wissa, H. H. Hassan, A. A. Ebnalwaled, and S. A. Khairy, "Enhanced photocatalytic activity of green synthesized zinc oxide nanoparticles using low-cost plant extracts," *Sci. Rep.*, vol. 14, no. 1, Jul. 2024, doi: 10.1038/s41598-024-66975-1.

[13] Hasiah, Demi Dama Yanti, and Bambang Ari Wahjoedi, "SINTESIS NANOPARTIKEL ZnO MENGGUNAKAN EKSTRAK DAUN MANGGA (Mangifera sp.) DAN STUDI APLIKASINYA SEBAGAI FOTODEGRADASI CONGO REDd," *ALOTROP*, vol. 9, no. 1, pp. 107–118, Jun. 2025, doi: 10.33369/alo.v9i1.40396.

[14] B. Qu, Z. Xiao, and Y. Luo, "Sustainable nanotechnology for food preservation: Synthesis, mechanisms, and applications of zinc oxide nanoparticles," *J. Agric. Food Res.*, vol. 19, p. 101743, Mar. 2025, doi: 10.1016/j.jafr.2025.101743.

[15] G. D. Sani, A. Yakubu, A. Saidu, S. Sahabi, and S. Abdullahi, "A Review on Industrial Applications of Zinc Oxide Nanoparticles," vol. 5, no. 1, 2023.

[16] N. M. Hosny, I. Gomaa, M. G. Elmahgary, and M. A. Ibrahim, "ZnO doped C: Facile synthesis, characterization and photocatalytic degradation of dyes," *Sci. Rep.*, vol. 13, no. 1, Aug. 2023, doi: 10.1038/s41598-023-41106-4.

[17] J. Silver, S. Lubis, and M. Ramli, "Green Synthesis, Characterization, and Photocatalytic Activity of Zinc Oxide Nanoparticles on Photodegradation of Naphthol Blue Black Dye," *J. Kim. Sains Dan Apl.*, vol. 26, no. 9, pp. 363–371, Dec. 2023, doi: 10.14710/jksa.26.9.363-371.

[18] "Zinc Oxide Nanoparticles Synthesis Methods and its Effect on Morphology: A Review," *Biointerface Res. Appl. Chem.*, vol. 12, no. 3, pp. 4261–4292, Aug. 2021, doi: 10.33263/briac123.42614292.

[19] H. Nasir, S. K. Zahra, A. Khan, * A., and S. Naheed, "A REVIEW OF SUSTAINABLE METHODS FOR SYNTHESIZING ZINC OXIDE NANOPARTICLES AND THEIR APPLICATIONS," *Sci. Herit. J.*, vol. 8, no. 1, pp. 27–37, Dec. 2023, doi: 10.26480/gws.01.2024.27.37.

[20] B. Naiel, M. Fawzy, M. W. A. Halmy, and A. E. D. Mahmoud, "Green synthesis of zinc oxide nanoparticles using Sea Lavender (Limonium pruinosum L. Chaz.) extract: characterization, evaluation of anti-skin cancer, antimicrobial and antioxidant potentials," *Sci. Rep.*, vol. 12, no. 1, p. 20370, Nov. 2022, doi: 10.1038/s41598-022-24805-2.

[21] E. Aprilianto, A. V. Harmoni Swantika Yuan, C. D. Pradita, and P. Hendra, "Anti-inflammatory effects of avocado peels against inflammation induced by carrageenan in mice," *Pharmaciana*, vol. 9, no. 2, p. 219, Nov. 2019, doi: 10.12928/pharmaciana.v9i2.13607.

[22] N. Saridewi, A. R. Adinda, and S. Nurbayti, "Characterization and Antibacterial Activity Test of Green Synthetic ZnO Nanoparticles Using Avocado (Persea americana) Seed Extract," *J. Kim. Sains Dan Apl.*, vol. 25, no. 3, pp. 116–122, Mar. 2022, doi: 10.14710/jksa.25.3.116-122.

[23] S.P. Vinay, N. Chandrashekar, and C.P. Chandrappa,"Silver nanoparticles: Synthesized by leaves extract of Avocado and their antibacterial activity," *International Journal of Engineering and Research*. vol. 5, no. 2, 2017.

[24] S. Vijayakumar, B. Vaseeharan, B. Malaikozhundan, and M. Shobiya, "Laurus nobilis leaf extract mediated green synthesis of ZnO nanoparticles: Characterization and biomedical applications," *Biomed. Pharmacother.*, vol. 84, pp. 1213–1222, Dec. 2016, doi: 10.1016/j.biopha.2016.10.038.

[25] B. Kumar and L. Cumbal, "UV-Vis, FTIR and antioxidant study of Persea Americana (Avocado) leaf and fruit: A comparison," . . ., 1869.

[26] D. Mutukwa, R. Taziwa, and L. E. Khotseng, "A Review of the Green Synthesis of ZnO Nanoparticles Utilising Southern African Indigenous Medicinal Plants," *Nanomaterials*, vol. 12, no. 19, p. 3456, Oct. 2022, doi: 10.3390/nano12193456.

[27] A. A. Alshehri and M. A. Malik, "Biogenic fabrication of ZnO nanoparticles using Trigonella foenum-graecum (Fenugreek) for proficient photocatalytic degradation of methylene blue under UV irradiation," *J. Mater. Sci. Mater. Electron.*, vol. 30, no. 17, pp. 16156–16173, Sep. 2019, doi: 10.1007/s10854-019-01985-8.

[28] P. L. Meena, P. Bhardwaj, Y. Kumar, and S. P. Singh, "Synthesis and characterization of one dimensional ZnO nanorods," in *AIP Conference Proceedings*, Longowal, India: AIP Publishing, 2021, p. 040043. doi: 10.1063/5.0053072.

[29] M. Lal, P. Sharma, and C. Ram, "Optical, structural properties and photocatalytic potential of Nd-ZnO nanoparticles synthesized by hydrothermal method," *Results Opt.*, vol. 10, p. 100371, Feb. 2023, doi: 10.1016/j.rio.2023.100371.

[30] K. Davis, R. Yarbrough, M. Froeschle, J. White, and H. Rathnayake, "Band gap engineered zinc oxide nanostructures *via* a sol–gel synthesis of solvent driven shape-controlled crystal growth," *RSC Adv.*, vol. 9, no. 26, pp. 14638–14648, 2019, doi: 10.1039/c9ra02091h.

[31] B. Gherbi *et al.*, "Effect of pH Value on the Bandgap Energy and Particles Size for Biosynthesis of ZnO Nanoparticles: Efficiency for Photocatalytic Adsorption of Methyl Orange," *Sustainability*, vol. 14, no. 18, p. 11300, Sep. 2022, doi: 10.3390/su141811300.

[32] S. Adesoye, S. Al Abdullah, K. Nowlin, and K. Dellinger, "Mg-Doped ZnO Nanoparticles with Tunable Band Gaps for Surface-Enhanced Raman Scattering (SERS)-Based Sensing," *Nanomaterials*, vol. 12, no. 20, p. 3564, Oct. 2022, doi: 10.3390/nano12203564.

[33] P. Makuła, M. Pacia, and W. Macyk, "How To Correctly Determine the Band Gap Energy of Modified Semiconductor Photocatalysts Based on UV–Vis Spectra," *J. Phys. Chem. Lett.*, vol. 9, no. 23, pp. 6814–6817, Dec. 2018, doi: 10.1021/acs.jpclett.8b02892.

[34] O. M. A. Halim *et al.*, "A review on modified ZnO for the effective degradation of methylene blue and rhodamine B," *Results Surf. Interfaces*, vol. 18, p. 100408, Jan. 2025, doi: 10.1016/j.rsurfi.2024.100408.

[35] D. Nzilu *et al.*, "Synthesis and Characterization of Parthenium hysterophorus-Mediated ZnO Nanoparticles for Methylene Blue Dye Degradation," *J. Chem.*, vol. 2024, pp. 1–19, Jan. 2024, doi: 10.1155/2024/1088430.

[36] A. Kulis-Kapuscinska *et al.*, "Photocatalytic degradation of methylene blue at nanostructured ZnO thin films," *Nanotechnology*, vol. 34, no. 15, p. 155702, Apr. 2023, doi: 10.1088/1361-6528/aca910.

[37] M. H. Shakoor *et al.*, "Enhancing the Photocatalytic Degradation of Methylene Blue with Graphene Oxide-Encapsulated g-C_3N_4/ZnO Ternary Composites," *ACS Omega*, vol. 9, no. 14, pp. 16187–16195, Apr. 2024, doi: 10.1021/acsomega.3c10172.